The 2013 World Congress on
Advances in Structural Engineering and Mechanics (ASEM13)
Jeju, Korea, September 8-12, 2013

Deformation behavior of the granular materials in the surface layer accompanying the reverse fault of the bedrock

*Shigeaki NOZOE[1)]Kenji KANEKO[2)] Yutaka HASHIZUME[3)] and Msahiko EBARA[4)]

[1), 2), 3)] *Department of Civil Engineering, Hachinohe Institute of Technology, Aomori, Japan*
[3)] *Department of Civil Engineering, Electric Power Development Co., Ltd. Tokyo, Japan*
[2)] *kaneko@hi-tech.ac.jp*

ABSTRACT

We have aimed to develop a method to prevent destruction of the earth structures by dip-slip fault. In this study, we carried out the development of the centrifugal experimental apparatus to investigate the fundamental knowledge about the deformation behavior of granular media upon the dip-slip fault. Using the developed dip-slip apparatus, we carried out some experiments in a 100G situation. The results of tests indicated that the progressive direction of the shear band depends on the confining pressure.

1. INTRODUCTION

Discussion of structural damages caused by the earthquake has been performed on the ground motion mainly. However, a structure may suffer a serious damage also from the foundation displacement by the slip of a fault. Particularly, in the case of the dip-slip fault, the vertical displacement of the ground surface, which sometimes reaches several meters, leads to the collapse of the structures. For example, at the 1999 Chi-Chi earthquake, many infrastructures suffered damage from displacement by dip-slip fault. On the other hand, geological study of the fault has developed. And many information including the position of a fault, the failure form and the probability of motion have come to be acquired. Thereby, established important structures just on the active fault increased in Japan. We need to estimate the deformation and the failure of structures with accuracy and to develop a countermeasure method. However, we have not understood the deformation and the failure of the soil structures due to the large displacement of the foundation by the dip-slip fault clearly.

In this study, to target as the high embankment such as the fill dam at the top of the dip-slip fault, performing fundamental experiments for predicting the deformation behavior when a fault occurs. In particular, we consider such as the position of shear zones and the amount of displacement of the ground surface of the dip-slip fault occurs,

[1)] Graduate Student
[2)] Associate Professor
[3)] Post Doctoral Fellow
[4)] Master of Engineering

discontinuous surface reaches to the ground surface and development.

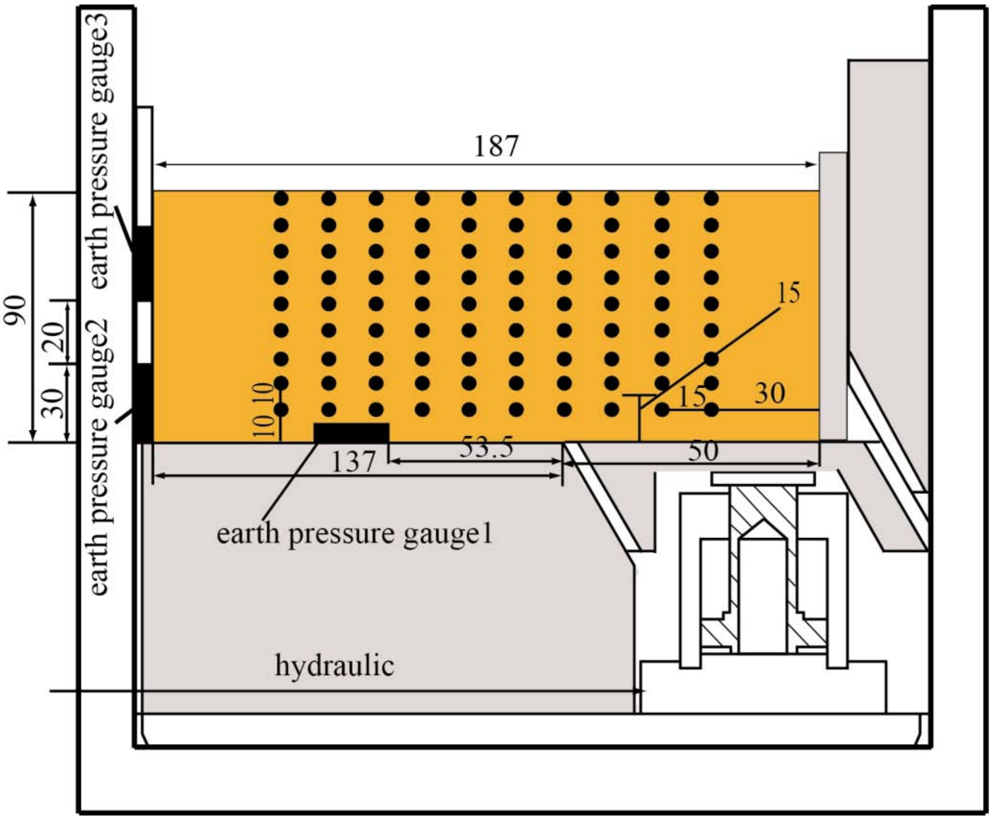

Fig. 1 Schematic diagram of test device of a dip-slip fault

2. OUTLINE OF DIP-SLIP FAULT MODEL TEST

Although most of the experimental study to investigate the deformation characteristics of soil layer upon the dip-slip fault is performed in the 1G situation, it is very difficult to reproduce a large confining pressure acted on high embankment. In this study, in order to perform the dip-slip experiments with high confining pressure, we develop the new experimental device by using centrifugal loading apparatus. A diagram of the developed experimental device is illustrated in Fig. 1. We can regard the thickness of soil layer as 9m in the 100G situation, but the real thickness is 90mm. We represent the dip-slip fault by giving the displacement to the part of 50mm from the right side. In this paper, we set the angle of fault to 75 degree.

The test box is made with steel, but only the front is made by a transparent acrylic plate to observe the deformation of soil layer. We install 90 targets to chase the displacements inside the soil layer. A state of the soil layer during the fault movement is photographed by a video camera. From the photographs, the displacement of the targets is obtained by image analysis. In addition, three earth pressure gauges are installed as in Fig. 1 to measure the variation of the earth pressure during the dip-slip motion.

Soil materials used in this experiments are a glass beads and silica sand No.5. The main difference of these materials is an internal friction angle. We use the materials in perfectly dry state. The properties and the grain size distributions of soil materials are shown in Tab. 1 and Fig. 2, respectively. We made the soil layer carefully by dividing into 9 layers to control the relative density as a constant value. We set the relative density to 50% in the case of all materials.

Table.1 Fundamental nature of the soil material

soil material	silica sand No.5	glass beads
ρ_s (g/cm^3)	2.68	2.489
D_{50}	0.55	0.44
U_c	1.31	1.3
U'_c	1.31	0.947
ρ_{dmin} (g/cm^3)	1.304	1.450
ρ_{dmax} (g/cm^3)	1.601	1.579
c_d (kN/m^2)	5	0
ϕ_d(°)	38.9	31.9

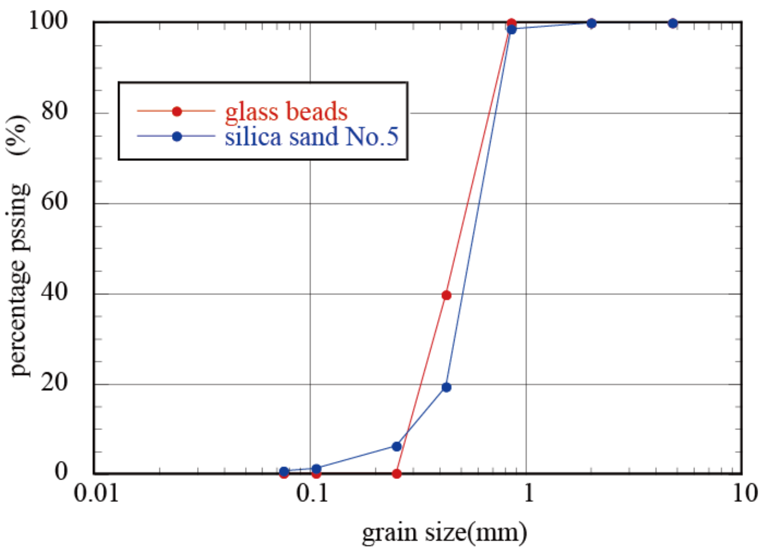

Fig. 2 Grain size distribution curve

3. EXPERIMENTAL RESULTS

3.1 Displacements of the inside the soil layer

We got the position coordinates of the targets installed into soil layer by analyzing the image capture obtained during the experiments. As an example, Fig. 3 shows the position coordinates of targets in the initial state and fainal one. In this figure, we show also the extended line, which is inclined 75 degree, from the boundary point of the dip-slip fault of bedrock. In the case of glass beads, the soil on the right hand side of the line is displaced approximately rigidly, on the other hand the soil without near the ground surface on the left hand side is not displaced. In the case of silica sand, we can observe that the soil on the left hand side is displaced comparatively. In the both case, horizontal displacement tends to increase so as to approach the earth surface whose confining pressure is small.

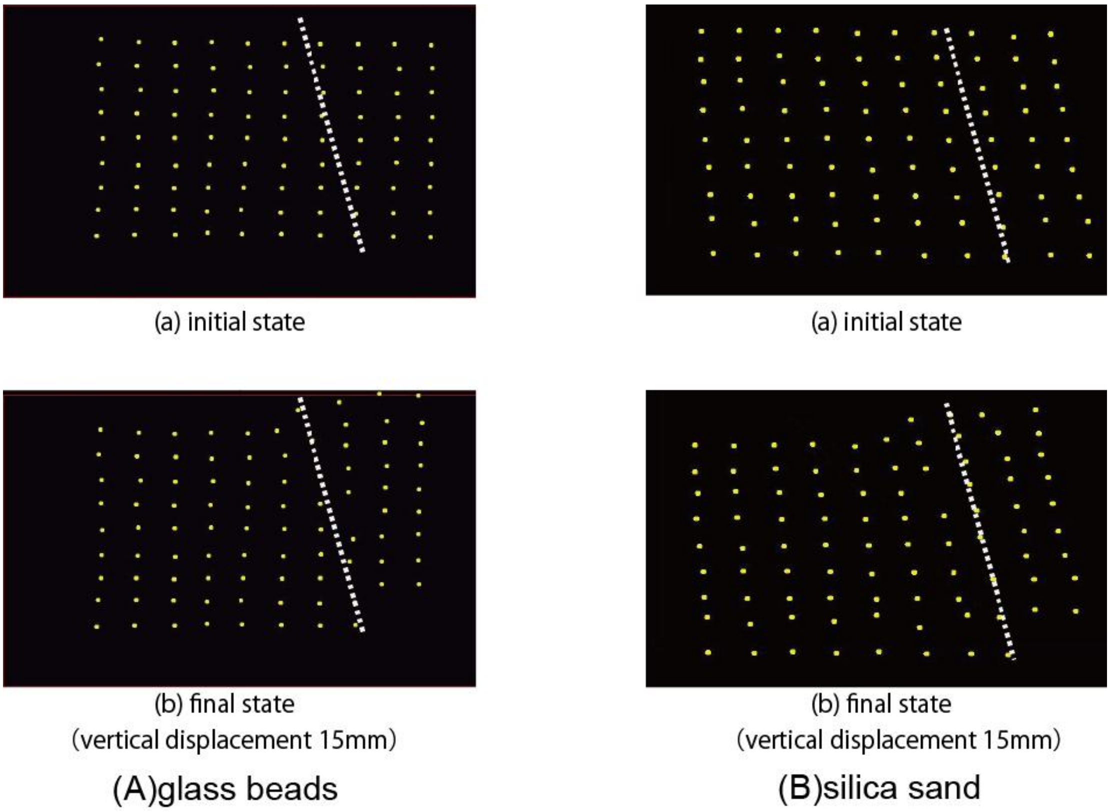

Fig. 3 Initial and final position coordinates of the target

Figure. 4 shows the positional coordinates of the targets in the ground surface after the dip-slip fault (vertical displacement 15mm). In the position where the compulsory displacement of bedrock reaches the surface, the case of the silica sand whose internal friction angle is larger than glass beads becomes the left side. It is important task in the future that we will investigate the relationship between the deformation characteristics and the internal friction angle of soil materials in detail.

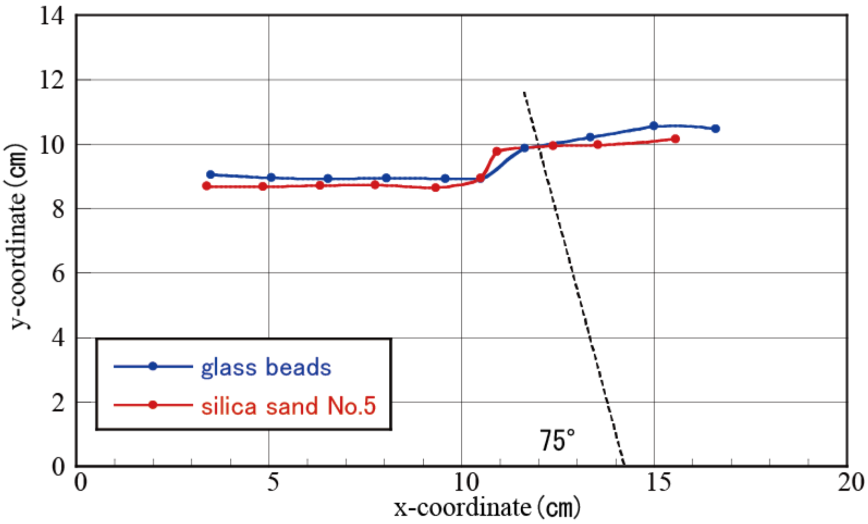

Fig. 4 Position of the ground surface due to the dip-slip fault

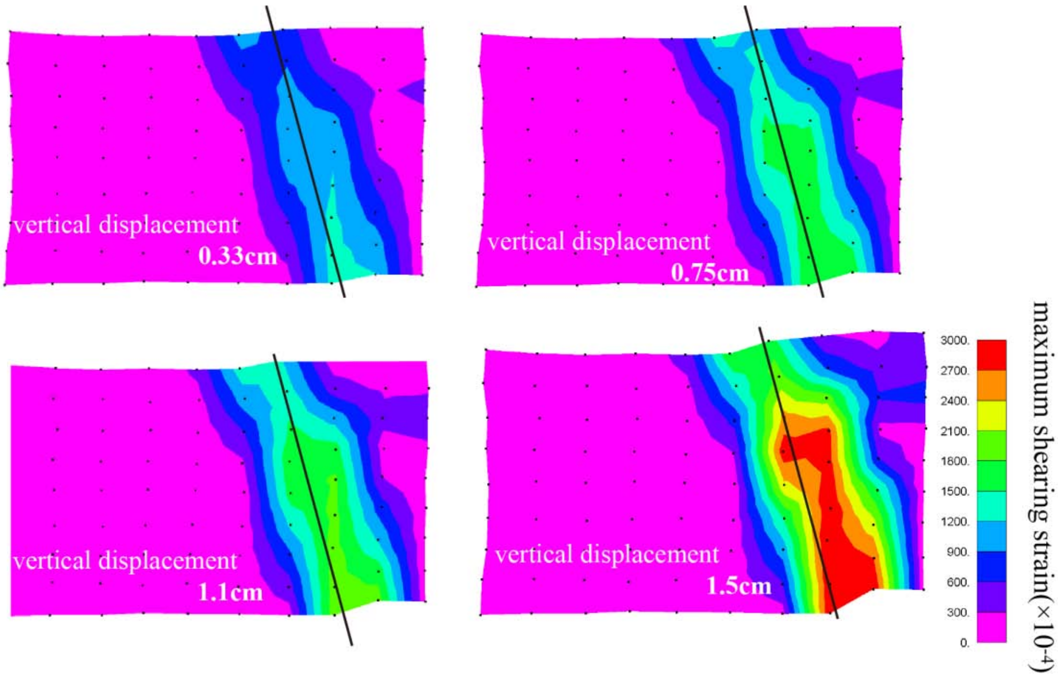

Fig. 5 Maximum shear strain distribution (glass beads)

3.2 Strain distribution

Next, we calculated strains inside the soil layer by considering the targets, which was obtained by experiments, as the nodes of a finite element. We reconfigure the elements at each step, because there is a possibility that the element is improper large deformation due to the large displacement of bedrock. Then, we computed the incremental strain in each image step and add them.

The maximum shear strain distribution in the case of a glass beads is illustrated in Fig. 5. Although the accuracy is not so good because of the number of targets, we can observe in this figure that a shear band is gradually developed along with the progress of the fault. The development of the shear zone begins from neighborhood of the boundary between the upper and the lower wall of the fault. The shear zone slips off on the left side so as to approach the surface. We can consider from these results that the progress direction of the shear zone depends on the confining pressure. Moreover, we can observe that the bifurcation of the shear band occurs. However, the strain level in the bifurcated shear zone is relatively small.

Figure 6 shows the volumetric strain distribution. From the distribution of volume strain, the existence of the volume dilation around shear zone can be confirmed. Since permeability may improve by the dilation, our attention is necessary in the soil structures made for the purpose of stopping water such as the fill dam.

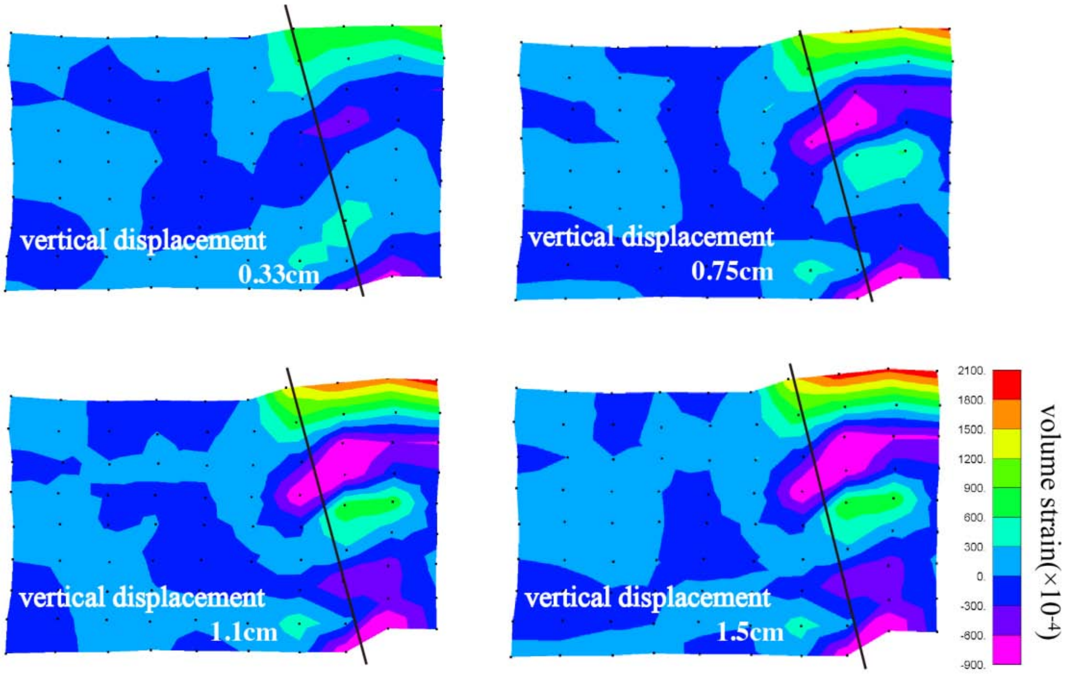

Fig. 6 Volumetric strain distribution (glass beads)

3.3 Horizontal and vertical earth pressure

Fig. 7 shows the variation of earth pressure, which is measured by earth pressure gauges during the experiment. Time on the horizontal axis is the time from the start of centrifugal loading. A vertical earth pressure grows along with the rise of the centrifugal force. Also, the vertical earth pressure at the centrifugal acceleration 100G, is in agreement with the theoretical value calculated on the basis of the density of the soil. The horizontal earth pressure increases a little with increase in the displacement of the dip-slip fault of bedrock. Because the horizontal earth pressures increase with the fault occurs, we can’t ignore the influence of horizontal boundary condition. If we will assume the semi-infinite ground, there is the possibility that the volume dilation around the shear band occur larger than these experimental results. It will be necessary to examine influence of the boundary condition to give the deformation behavior of soil layer by the displacement of the bedrock.

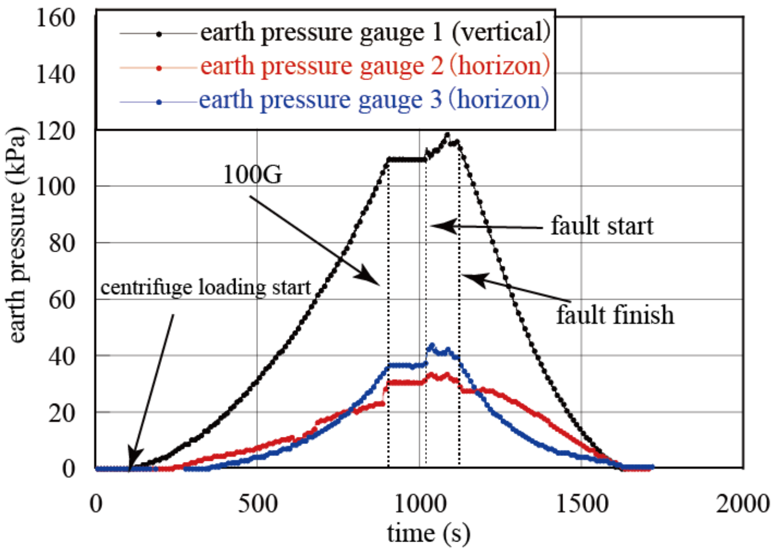

Fig. 7 Variation of the earth pressures with the fault (glass beads)

4. CONCLUSION

In this study, we developed the test device to investigate the deformation behavior of the high embankment due to the dip-slip fault by using centrifugal loading equipment. Using the developed test device, we carried out the some experiments. We could observe the shear band and the volume change from the results of the test. However, because the deformation behavior of soil layer with the large displacement of the bedrock fault is influenced by many factors, it is necessary to increase the experimental results in the future.

REFERENCES

Horsfield, W.T., (1977), “An experimental approach to basement controlled faulting”, *Geologie en mijnbouw.,* **56**(4), 363-370.

Tsuneishi, Y., (1978), “Geological and experimental studies on mechanism of block faulting”, *Bull. Earthq. Res. Inst.,* **53**, 173-242.

Roth, W.H., R.F. Scott and I. Austin., (1981), “Centrifuge modeling of fault propagation through alluvial soils”, *Geophys. Res. Lett.,* **8**(6), 561-564.

Cole, D.A.Jr. and Lade, P.V., (1989), “Influence zones in alluvium over dip-slip faults”,*J Geotech.Eng., ASCE,* **110**(5), 599-615.

Naylor, M.A., Mandl, G. & Sijipesteijin., (1986), “Fault geometries in basement-induced wrench faulting under different initial stress states”, *J. Struct. Geol.,* **8**(7), 737-752.

Bray, J.D., R.B. Seed and H.B. Seed., (1994), “Analysis of earthquake rupture propagation through cohesive soil”, *J. Geotech.Engerg., ASCE,* **120**(3), 562-580.